edged. We also wish to thank Professor Dave Russell, Mr. Vincent Oriedo, and Professors Peter Armentrout and Jim Weisshaar for communicating results prior to publication and for several useful discussions. Finally, we wish to acknowledge Gert von Helden for writing the arrival time peak shape fitting program used to determine Fe^+ $3d^64s^1$ and $3d^7$ populations and the $3d^7$ to $3d^64s^1$ deactivation rate constant.

Appendix: Solution of Kinetic Equations for $Fe^+ + C_3H_8$

In order to calculate the theoretical product distributions, the kinetics of each state must be solved. In the derivation "**" refers to the ^4D second excited state, "*" to the ^4F first excited state, and no asterisks to the ground state.

(1) For the ^4D $4s3d^6$ second excited state, $(Fe^+)^{**}$, it is assumed that no deactivation occurs (analogous the $4s3d^7$ excited states of Co^+). This implies that the fractional decrease $(Fe^+)^{**}/(Fe^+)_0^{**}$ of this state is a simple exponential decay given in eq A1a. The total products, $(P^+)^{**}$ and the elimination products, $(P^+)_e^{**}$, formed as a function of time are given in eqs A1b and A1c, respectively.

$$(Fe^+)^{**} = (Fe^+)_0^{**}e^{-k_{tot}^{**}t} \qquad k_{tot}^{**} = k_e^{**} + k_a^{**} \tag{A1a}$$

$$(P^+)^{**} = (Fe^+)_0^{**}(1 - e^{-k_{tot}^{**}t}) \tag{A1b}$$

$$(P^+)_e^{**} = (Fe^+)_0^{**}(k_e^{**}/k_{tot}^{**})(1 - e^{-k_{tot}^{**}t}) \tag{A1c}$$

In these equations, k_e^{**}, k_a^{**}, and k_{tot}^{**} correspond to the rate constants for elimination, adduct formation, and the total rate constant for the ^4D second excited state reacting with propane. The rate constants have units of s^{-1} and are equal to the bimolecular rate coefficient times the reactant concentration ($k_e^{**} = k_{H_2}(C_3H_8) + k_{CH_4}(C_3H_8)$ and $k_a^{**} = k_3(He)(C_3H_8)$).

(2) For the ^4F first excited state $(Fe^+)^*$, rapid deactivation to the ground state occurs. The fractional decrease $(Fe^+)^*/(Fe^+)_0^*$ for this state is again a simple exponential decay given in eq A2a. In this case, however, k_{tot}^*, which is the sum of the rates of deactivation, elimination, and adduct formation, can be approximated by the rate of deactivation k_d^* (bimolecular deactivation rate times the He concentration). The elimination products, $(P^+)_e^*$, formed as a function of time are given in eq A2b.

$$(Fe^+)^* = (Fe^+)_0^*\, e^{-k_{tot}^*t} \qquad k_{tot}^* = k_a^* + k_e^* + k_d^* \approx k_d^* \tag{A2a}$$

$$(P^+)_e^* = (Fe^+)_0^*(k_e^*/k_{tot}^*)(1 - e^{-k_{tot}^*t}) \tag{A2b}$$

For reaction times greater than 100 μs, the ^4F state has been completely deactivated and the products formed prior to deactivation are constant and independent of time, eq A3.

$$(P^+)_e^* = (Fe^+)_0^*(k_e^*/k_d^*) = \text{constant} \tag{A3}$$

(3) The ^6D ground state reacts away to form the adduct and eliminate H_2 and CH_4 but is produced in the deactivation of the ^4F state as shown in eq A4, the solution to which is given in eq A5.

$$d(Fe^+)/dt = -k_{tot}(Fe^+) + k_d^*(Fe^+)^* \tag{A4}$$

$$(Fe^+) = (Fe^+)_0e^{-k_{tot}t} + \frac{(Fe^+)_0^*k_d^*}{k_{tot} - k_d^*}[e^{-k_d^*t} - e^{-k_{tot}t}] \tag{A5}$$

The total products for ground-state Fe^+ reacting with propane are calculated using expression A6 which has the solution given

$$d(P^+)/dt = k_{tot}(Fe^+) \tag{A6}$$

by expression A7. The elimination products, $(P^+)_e$, formed from ground-state Fe^+ as a function of time are given in eq A8. Under our experimental conditions, $k_{tot} \le k_d^*/200$ and $k_{tot} - k_d^* \approx -k_d^*$. In addition, for reaction times, $t > 10^{-4}$ s, $e^{-k_d^*t} < 10^{-3}$ and eqs A7 and A8 simplify to expressions A9 and A10, respectively.

$$(P^+) = (Fe^+)_0(1 - e^{-k_{tot}t}) + \frac{(Fe^+)_0^*k_d^*k_{tot}}{k_{tot} - k_d^*}\left[\frac{(1 - e^{-k_d^*t})}{k_d^*} - \frac{(1 - e^{-k_{tot}t})}{k_{tot}}\right] \tag{A7}$$

$$(P^+)_e = (Fe^+)_0\frac{k_e}{k_{tot}}(1 - e^{-k_{tot}t}) + \frac{(Fe^+)_0^*k_d^*k_e}{k_{tot} - k_d^*}\left[\frac{(1 - e^{-k_d^*t})}{k_d^*} - \frac{(1 - e^{-k_{tot}t})}{k_{tot}}\right] \tag{A8}$$

$$(P^+) = [(Fe^+)_0 + (Fe^+)_0^*](1 - e^{-k_{tot}t}) - (Fe^+)_0^*(k_{tot}/k_d^*) \tag{A9}$$

$$(P^+)_e = [(Fe^+)_0 + (Fe^+)_0^*]\frac{k_e}{k_{tot}}(1 - e^{-k_{tot}t}) - (Fe^+)_0^*\frac{k_e}{k_d^*} \tag{A10}$$

At this point, the total products eliminated from all three electronic states of Fe^+ reacting with propane can be calculated as a function of reaction time. The elimination rate constant of the ^4F state, k_e^*, is used as the only variable parameter to fit the experimental data.

Communications to the Editor

In Situ Chemisorption-Induced Reordering of Oxidatively Disordered Pd(100) Electrode Surfaces

John R. McBride, Jane A. Schimpf, and Manuel P. Soriaga*,†

Department of Chemistry, Texas A&M University College Station, Texas 77843

Received September 11, 1992

The regeneration of ordered, well-defined electrode surfaces outside an ultra-high vacuum environment is of utmost concern in electrochemical surface science. Four methods have been suggested in the past.[1-5] Three[1-4] require high-temperature treatments outside the electrochemical cell. The fourth method,[5] based upon microscopic electropolishing, is limited to reactive metals. Recently, we discovered that an oxidatively disordered Pd(111) surface could be reordered under purely electrochemical conditions.[6,7] The reordering is based upon the formation of a stable, highly ordered iodine overlayer when a Pd(111) single-

* Author to whom correspondence should be addressed.
† Presidential Young Investigator.

(1) Clavilier, J. *J. Electroanal. Chem.* **1980**, *107*, 211.
(2) Motoo, S.; Furuya, N. *J. Electroanal. Chem.* **1984**, *172*, 339.
(3) Wieckowski, A.; Schardt, B. C.; Rosasco, S. D.; Stickney, J. L.; Hubbard, A. T. *Inorg. Chem.* **1984**, *23*, 565.
(4) Zurawski, D.; Rice, L.; Hourani, M.; Wieckowski, A. *J. Electroanal. Chem.* **1987**, *230*, 221.
(5) Stickney, J. L.; Villegas, I.; Ehlers, C. B. *J. Am. Chem. Soc.* **1989**, *111*, 6473.
(6) Rodriguez, J. F.; Bothwell, M. E.; Cali, G. J.; Soriaga, M. P. *J. Am. Chem. Soc.* **1990**, *112*, 7392.
(7) Cali, G. J.; Berry, G. M.; Bothwell, M. E.; Soriaga, M. P. *J. Electroanal. Chem.* **1991**, *297*, 523.

0002-7863/92/1514-10950$03.00/0

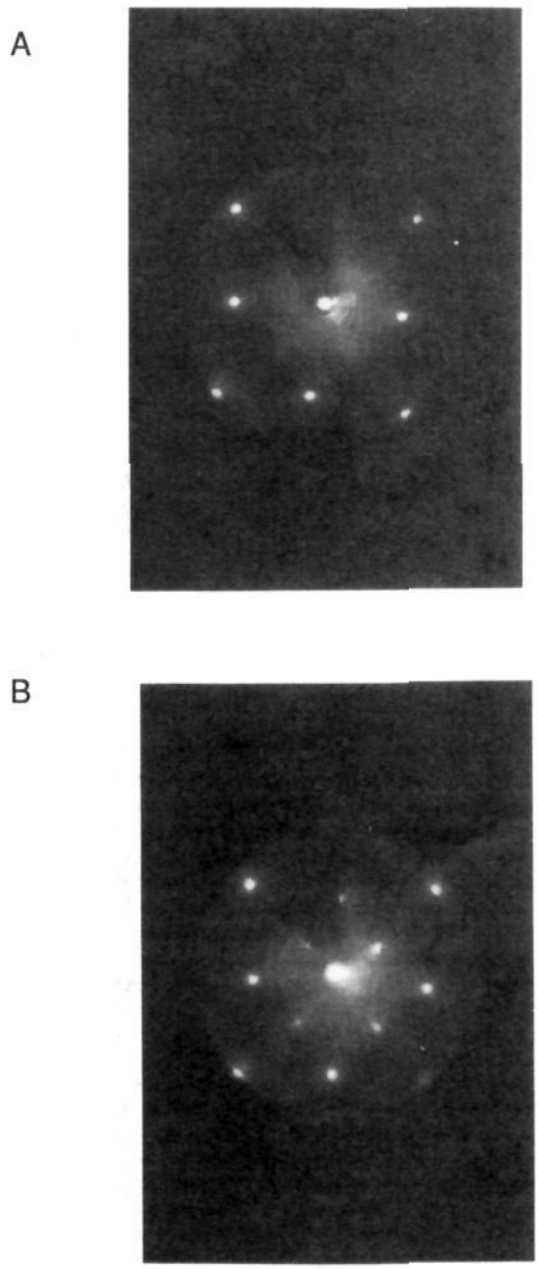

Figure 1. Low-energy electron diffraction (LEED) pattern for a clean and ordered Pd(100) single-crystal electrode before (A) and after (B) exposure to 0.5 mM NaI at pH 10. Beam energy = 60 eV; beam current = 2 μA.

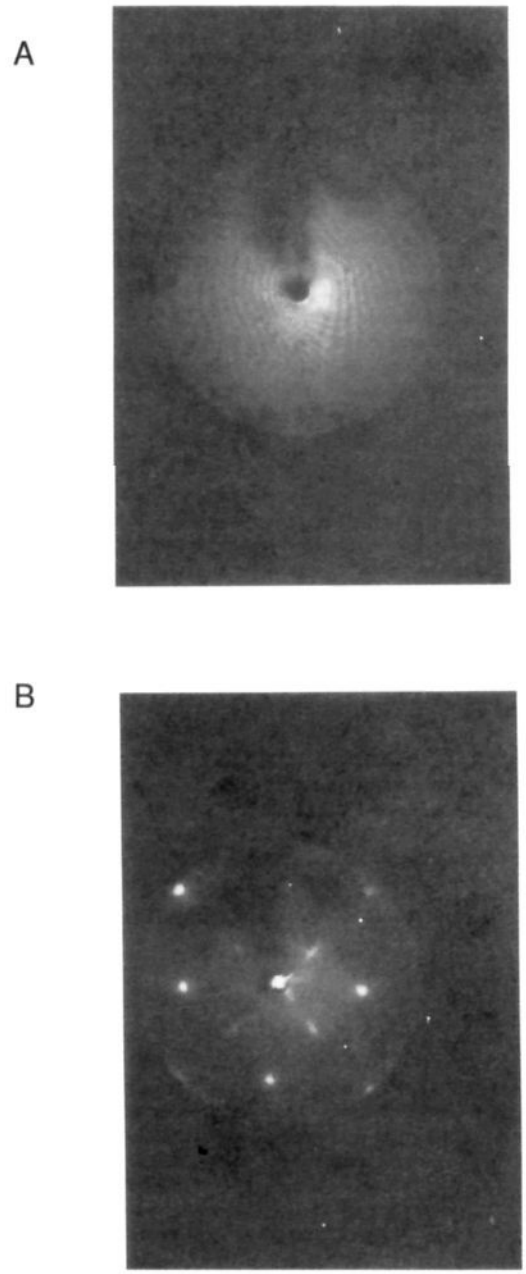

Figure 2. LEED pattern for a fully oxided Pd(100) surface before (A) and after (B) reduction at potentials just prior to hydrogen evolution in the presence of 0.5 mM NaI at pH 10. Experimental conditions were as in Figure 1.

crystal electrode previously disordered by electrochemical oxidation is exposed, at room temperature and at potentials within the double-layer region, to an alkaline solution of NaI. It is fundamentally important to ascertain whether this phenomenon is general or is limited only to the (111) crystallographic plane. In this communication, we present new results which demonstrate that adsorption-induced disorder-to-order interfacial reconstruction also occurs at an anodically disordered Pd(100) electrode surface.

Our experiments were performed in an ultra-high vacuum chamber equipped with low-energy electron diffraction (LEED) optics, a cylindrical mirror analyzer for Auger electron spectroscopy (AES), and an isolable compartment for electrochemical experiments.[8] Initial preparation of a clean and atomically smooth Pd(100) surface involved a few weeks of sequential O_2(g) oxidations, Ar^+ ion bombardment, and thermal annealing to remove traces of Si, P, and S bulk impurities. Electrolytic solutions (Millipore Milli-Q water) contained 0.1 M NaF adjusted to pH 10 with NaOH; iodine chemisorption was from 0.5 mM NaI at the same supporting electrolyte. An alkaline solution was chosen to ensure that acid-induced dissolution would not occur.

Figure 1A shows the LEED pattern for a clean and ordered Pd(100) single crystal. The presence of the sharp (1×1) integral index spots demonstrate the long-range order of the surface. The LEED pattern which results when the Pd(100) surface is exposed to dilute NaI at pH 10 is shown in Figure 1B. The distinct diffraction spots indicate the existence of an ordered adlayer of chemisorbed I atoms. Combined analysis of the LEED and AES data suggests the formation of a Pd(111)c(2X2)–I [Pd(100)-($\sqrt{2}$X$\sqrt{2}$)R45°–I] adlattice.

It is known that anodic oxidation disorders the electrode surface, primarily due to place-exchange reactions.[9] Long-range order

(8) Soriaga, M. P. *Prog. Surf. Sci.* **1992**, *39*, 325.

(9) Angerstein-Kozlowska, H.; Conway, B. E.; Sharp, W. B. A. *J. Electroanal. Chem.* **1973**, *9*, 1973.

is not necessarily reestablished even after the oxided electrode is reduced back to the metal. Figure 2A shows the result of the LEED experiment performed after extensive anodic oxidation of the Pd(100) electrode; the absence of discernible LEED spots betrays the high degree of disorder of the oxided surface. Figure 2B shows the LEED pattern generated when the oxide-coated Pd(100) electrode was immersed, at room temperature and at potentials where the metal oxide is reduced, in a solution of 0.5 mM NaI at pH 10. It is easy to see that this LEED pattern is identical to that for the initially ordered Pd(100) electrode (Figure 1B). The Auger spectrum for the reordered interface is likewise identical with that for the unoxidized surface. It is thus clear that the oxided, disordered Pd(100) surface has been reordered by electrochemical reduction and subsequent iodine chemisorption. Since the reordering occurs under conditions where Pd dissolution is negligible,[10] the driving force for this disorder-to-order surface reconstruction is most probably the formation of the highly stable Pd(100)c(2×2)-I adlattice.

The present results demonstrate that the in situ regeneration of clean and ordered single-crystal electrode surfaces from the simple sequence of oxidation, reduction, and iodine chemisorption, first reported by us for Pd(111),[6,7] is also applicable to Pd(100). The iodine-free single-crystal surface could then be prepared according to published procedures.[4,7] On-going studies are aimed at (i) exploring the applicability of the iodine–chemisorption reordering method to other electrode surfaces and (ii) identifying other reagents which can effect this in situ chemisorption-induced reordering phenomenon.

Acknowledgment. Acknowledgement is made to the National Science Foundation (Presidential Young Investigator program, DMR-8958440) and the Robert A. Welch Foundation for support of this work.

Registry No. Pd, 7440-05-3; I_2, 7553-56-2; NaI, 7681-82-5.

(10) McBride, J. R.; Soriaga, M. P. *J. Electroanal. Chem.* **1991**, *303*, 255.

$InMnO_3$: A New Transition Metal Oxide with an Unusual ABO_3 Structure

Daniel M. Giaquinta and Hans-Conrad zur Loye*

Department of Chemistry
Massachusetts Institute of Technology
Cambridge, Massachusetts 02139

Received August 24, 1992

We report the synthesis and structure of a new, unusual indium manganese oxide, $InMnO_3$, with a hexagonal layered structure containing manganese in trigonal bipyramidal coordination. Several common ABO_3 structural types are known, such as perovskite, corundum, ilmenite, and bixbyite,[1-9] and radius ratio rules, such as Goldschmidt's tolerance factor,[10] will generally predict which structural type will form for any given pair of cations. Two common ABO_3 structural families are characterized by (1) A and B cations of approximately equal size and of a size suitable for octahedral coordination by oxygen and (2) an A cation comparable in size to O^{2-}, which together with oxygen can form AO_3 closest-packed layers.[11] Oxides of the first group tend to adopt sesquioxide structures, such as corundum (α-Al_2O_3)[8,11] (a random distribution of cations in octahedral interstices, preferred by cations having the same oxidation state and/or similar radii) or ilmenite[12,13] (an ordered cation distribution preferred by cations having different oxidation states and/or different radii). Oxides of the second group form linked BO_6 octahedra and AO_3 closest-packed layers, such as perovskite,[1,2] $BaNiO_3$,[14] or hexagonal $BaTiO_3$ type structures,[15] as well as uncommon structural types,[16,17] e.g., the tunnel structure of $KSbO_3$.[18,19] $InMnO_3$, intriguingly, is not a member of these known structural families.

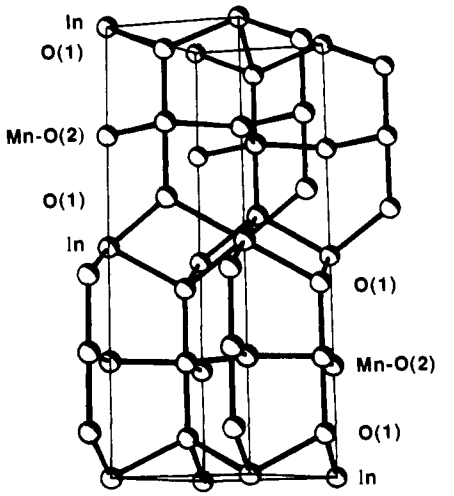

Figure 1. PLUTO drawing of the structure of $InMnO_3$. Selected bond lengths are In–O(1) = 2.202 (3), In–O(2) = 2.869 (nonbonding), In–Mn = 3.4756 (1), Mn–O(1) = 1.870 (8), Mn–O(2) = 1.9621 (1), Mn–Mn = 3.3985 (2), In–In = 3.3985 (2) Å.

Table I

atom	x	y	z	B_{eq}
In	0	0	0	1.97 (5)
Mn	$^2/_3$	$^1/_3$	$^1/_4$	1.05 (6)
O(1)	$^2/_3$	$^1/_3$	0.0871 (07)	2.0 (2)
O(2)	0	0	$^1/_4$	1.5 (4)

The Goldschmidt tolerance factor, $t = (r_A + r_O)/(2)^{1/2}(r_B + r_O)$, where r_A, r_B, and r_O are the ionic radii of A, B, and O^{2-}, respectively, predicts the perovskite structure for $1 > t > 0.8$ and the ilmenite structure for $0.8 \geq t$. In_2O_3 and Mn_2O_3 are known in both the bixbyite (an anion deficient fluorite structure) and corundum structures, and consequently, one would expect an ABO_3 indium manganese oxide to form a derivative of one of those two structural types. Furthermore, the tolerance factor for $InMnO_3$ is 0.80, confirming that ilmenite, the ordered corundum structure, should form. It is therefore surprising to find $InMnO_3$ in this very simple, yet unusual, layered hexagonal structure with two different cation coordination environments: octahedral and trigonal bipyramidal.

* Author to whom all correspondence should be addressed.

(1) Galasso, F. S. *Structure, Properties and Preparation of Perovskite Type Compounds*; Pergamon Press: Oxford, 1969.
(2) Goodenough, J. B.; Longo, J. M. *Landolt-Bornstein Tabellen, New Series, III/4a*; Springer-Verlag: Berlin, 1970.
(3) Goodenough, J. B. *Prog. Solid State Chem.* **1971**, *5*, 145.
(4) Smyth, D. M. *Annu. Rev. Mater. Sci.* **1985**, *15*, 329.
(5) Rao, C. N. R. *Annu. Rev. Phys. Chem.* **1989**, *40*, 291.
(6) Yakel, H. L., Jr. *Acta Crystallogr.* **1955**, *8*, 394.
(7) Mouron, P.; Choisnet, J.; Abs-Wurmach, I. *Eur. J. Solid State Inorg. Chem.* **1989**, *26*, 35.
(8) Schneider, S. J.; Roth, R. S.; Waring, J. L. *J. Res. NBS* **1961**, *65A*, 345.
(9) Norrestam, R. *Acta Chem. Scand.* **1967**, *21*, 2871.
(10) Goldschmidt, V. M. *Mat.-Naturv. Kl.* **1926**, *2*, 117.
(11) Wells, A. F. *Structural Inorganic Chemistry*; Clarendon Press: Oxford, 1984.
(12) Newnham, R. E.; Fang, J. H.; Santoro, R. P. *Acta Crystallogr.* **1964**, *17*, 240.
(13) Chamberland, B. L.; Sleight, A. W.; Weiher, J. R. *J. Solid State Chem.* **1970**, *1*, 512.
(14) Takeda, Y.; Kanamaru, F.; Shi Madra, M.; Koizumi, M. *Acta Crystallogr.* **1976**, *B32*, 2464.
(15) Burbank, R.; Evans, H., Jr. *Acta Crystallogr.* **1948**, *1*, 330.
(16) Geller, S.; Curlander, P. J.; Jefferies, J. B. *Acta Crystallogr.* **1975**, *B31*, 2770.
(17) Longo, J. M.; Raccah, R. M.; Goodenough, J. B. *Mater. Res. Bull.* **1969**, *4*, 191.
(18) Hong, H. Y.; Kafalas, J. A.; Goodenough, J. B. *J. Solid State Chem.* **1974**, *9*, 345.
(19) Goodenough, J. B.; Kafalas, J. A. *J. Solid State Chem.* **1973**, *6*, 493.

0002-7863/92/1514-10952$03.00/0